



Influence of compression coil geometry in electromagnetic forming using experimental and finite element method

Manoj Soni^{1,2} · Meraj Ahmed² · Sanjay Kumar Panthi² · Surendra Kumar² · Khushwant Singh Gavel²

Received: 15 February 2021 / Accepted: 1 August 2021 / Published online: 13 August 2021
© The Author(s), under exclusive licence to Springer-Verlag London Ltd., part of Springer Nature 2021

Abstract

Electromagnetic forming process is a high velocity forming technique which is widely used in automotive and aerospace sectors for forming and joining metallic sheet/tubes. The geometrical structure of compression coil has significant effect on the performance of the system in terms of current output and deformation of workpiece. The present work aims to analyse the effect of structural parameters of compression coil like cross-section of turns (X), pitch circular diameter (PCD) and effective turn (n) using both experimental and numerical simulation. A bitter compression coil of variable geometrical structure has been considered to see the effect of its parameters by deforming an AA6061 tube experimentally. Parameters like magnetic field, velocity, Lorentz force, displacement and stress are difficult to measure experimentally but have significant indication on performance of the coil in EMF. The trends of numerically predicated parameters find good agreement with experimental deformation value of tube. The FE simulation is carried out to correlate deformation results. The results indicate that n has higher significance in performance of compression coil as compared to X and PCD of coil.

Keywords Electromagnetic forming (EMF) · Different types of coil geometry · Inductance (L) · Energy level · Current amplitude · Frequency · Process parameters · FEM simulation

1 Introduction

In the present scenario, demand for light-weight and high specific strength materials is continuously increasing mainly in automobile and aerospace sector in order to save cost and increase fuel efficiency. Joining of similar and dissimilar light weight metals and forming of sheet metal are sometimes challenging due to various associated problems. These problems can be addressed with the help of high velocity joining and forming technique like electromagnetic forming (EMF), electrohydraulic forming (EHF) etc. EMF is a high energy rate forming technique that is widely used for joining of similar/dissimilar metal parts, cutting, crimping and sheet metal forming of the parts. It can be utilized for both sheet and

tubular types of parts. Some of the major advantages of EMF process are enhanced formability, reduced wrinkling and controlled springback effect, better strain distribution in sheet metal forming, improvement in dimensional accuracy in forming, elimination of heat-affected zone in welding and its environment friendly nature etc. [1–4]. This technique can be used in almost all sectors like automobile, aerospace, medical, nuclear, air conditioning and home appliance industries [4]. Depending on application of the process, generally three types of coil are used. Compression coil is used to compress a tubular geometry in inward direction to either achieve a desired shape of the tube or joining it to another tube on rod placed inside the tube in overlapped condition. Similarly, expansion coil is used for expansion of tube. Flat forming coil is used for sheet metal forming of flat workpiece. All these coils are of spiral helical in nature. So, coil is the core part of the tooling in EMF process and its geometrical structure plays important role in improving the performance of EMF process.

In the past, several researchers have used finite element simulation and experimental methods for studying various aspects like coil design, effect of process parameters etc. in electromagnetic forming. A few initial work in EMF is discussed to review the evolution of the process. One of the

✉ Manoj Soni
soni44@gmail.com

¹ Academy of Scientific and Innovative Research (AcSIR), Ghaziabad 201002, India

² Council of Scientific and Industrial Research(CSIR)-Advanced Materials and Processes Research Institute (AMPRI), Bhopal 462026, India

early work reported in the area reveals preliminary design of expansion of coil and its effect on various parameters such as frequency of discharge, velocity, discharge current and pressure acting on the work-piece [5]. Further work by Lal et al. [6] proposed a theoretical analysis of current in a typical EMF circuit considering coil parameters such as inductance, resistance and frequency. After a brief pause in research work in the area for about a decade (in 70s and 80s), there was renewed interest because of availability of high speed computational facility and requirement of light weight material in various sectors. Some of the work related to processing of material and various aspect of effect of coil design in EMF is discussed in the following paragraph. Murata et al. [7] presented a tube forming method using a tapered coil and called it tube streaming method. Effect of various parameters such as energy discharged by capacitor bank, length of tube and position of tube on deformation and profile of streaming has been examined. Min et al. [8] developed a FEM model and analysed the formation of wrinkles on the tube wall in electromagnetic tube compression. The effect of different shapes of the mandrel on the tube compression was studied and the usage of mandrel that can reduce wrinkles in electromagnetic forming process was proposed. A FEM model proposed by Lee et al. [9] analysed pressure distribution on the coil and workpiece. Effect of elements types on the error in FEM simulation was studied. It proposed that decrease in size and increase in number of elements reduced error but it increases computational time. Zhang et al. [10] studied the effect of skin depth and magnetic pressure on the workpiece deformation. Work carried out by Lee et al. [11] gives relation between magnetic pressure and tube length. It established the optimum length of tube that gives maximum deformation. It was argued that the size of tube length should be equal to the coil length to obtain maximum pressure on the workpiece. Zang et al. [12] proposed E shaped coil and its effect on the magnetic field developed across the coil. The gap of the coil is also optimized. It was argued that the performance of E shaped coil is better than other general coils. Meriched et al. [13] proposed a flat coil design in electromagnetic sheet metal forming process. Azab et al. [14] worked on various FEM model for electromagnetic forming analysis and a comparative study was carried out amongst them. Numerous challenges involved in FEM analysis of electromagnetic forming are discussed. Haiping et al. [15] analysed the effect of current frequency on the deformation of AA-3003 tube using numerical simulation and compared the effect of different frequencies on deformation. Optimum frequency was determined to get the largest deformation. Mamalis et al. [16] proposed a FEM model for compression coil with stepped field shaper and flat coil for deforming a tube and sheet metal parts. Effect of charging voltage, magnetic flux and Lorentz force in electromagnetic forming process was analysed. Shrivastava et al. [17] optimized stand of distance, energy and thickness of tube

in electromagnetic forming and validated results of FE simulation with experimental one. Various parameters like magnetic field, velocity, Lorentz force, displacement and velocity associated with EMF process was also calculated using FE simulation and co-related with experimental results. Ahmed et al. [18] proposed concept of uniform and non-uniform coil for flat sheet metal forming. Parameters like magnetic field, Lorentz force etc. were analysed for both the coil and it was established that the non-uniform coil provides improved electromagnetic force for forming sheet metal. Arezoodar et al. [19] developed a FEM model for investigation effect of different parameters such as material property, peak current etc. on inward tube deformation. It was established that material property can affect the depth of deformation. Li et al. [20] proposed a FEM model for analysing electromagnetic forming of low conducting materials using a high conducting driver material and investigated the distribution of magnetic force variation. Cao et al. [21] investigated the effect of current frequency in electromagnetic sheet metal forming process using finite element method. The study showed that frequency varies according to the capacitance of the system and it affects displacement or deformation of the material. Frequency and skin depth have been optimized to obtain maximum deformation. Dond et al. [22] investigated the effect of field shaper on the electromagnetic field distribution in EMF. Experimental and numerical simulation was carried out and found that the usage of field shaper can increase field intensity by 5.6 times. It was also found that the distribution of magnetic pressure and flux density would be more uniform with the help of a field shaper. X. Zeng et al. (2020) [23] proposed a new technique to deform the aluminium alloy sheet using a single copper strip by imposing inverse current into the copper strip and workpiece. The FE simulation of deformation was also carried out and results were validated with experiments. Savadkoochian et al. [24] analysed the effect of various parameters such as tube thickness, die entrance radius, discharge current and energy on wrinkling and bead depth on aluminium AA7075-T6 tube compression in electromagnetic forming process and found that the bead depth and die entrance radius have been more effective on controlling wrinkling as compared to other parameters.

From the above literature review, it can be seen that a very negligible work has been carried out on establishing the effect of bitter coil structural geometry on electromagnetic forming of Al alloy tubes using finite element method. It is known fact that understanding the design of bitter coil structure is an important aspect in electromagnetic forming process for its improved performance. There are many parameters like magnetic field, Lorentz force, velocity, stress and strain distribution that are very difficult to obtain and analyse experimentally. Various aspect of bitter coil like pitch circular diameter (PCD), turn cross section (X) and effective turns (n) have huge effect on output current pulse of the system and thereby

effecting forming and joining of tubes of various materials. The present work studies the effect of variation in coil geometry structure on deformation and its correlation with various FE calculated parameters with experimental results. Four different combinations of PCD, X, n of coil are considered to analyse its effect on the process parameters such as magnetic field, deformation, velocity, Lorentz force, displacement and effective stress has been established. It mainly focuses on the effect of various numerically calculated parameters due to coil geometry variation on deformation of aluminium alloy AA6061 tube to understand processing of materials in EMF. FEM results have been validated with experimental results in terms of maximum deformation of the tube. Commercially available LS-Dyna software is used for FEM analysis of tube deformation in electromagnetic forming.

2 Material and methods

2.1 Materials

Effect of variation in coil geometry and its correlation with FEM calculated parameters are validated by experimentally deforming an aluminium alloy tube. Aluminium alloy is generally used in aerospace and automobile application due to light-weight and high specific strength. Aluminium alloy AA6061 has been used to perform the experimental work in the present study. The tubes are annealed at 350°C with holding time of two hours. The mechanical properties of AA6061 in terms of flow curve at both quasi-static and high strain rate are shown in Fig. 1. Strain rate for quasi-static condition is 0.1 s^{-1} and 4000 s^{-1} for high strain rate [25, 26]. The same flow curve has been used in finite element analysis. Copper is used for fabrication of coil and field shaper. Chemical composition of AA6061 alloy is

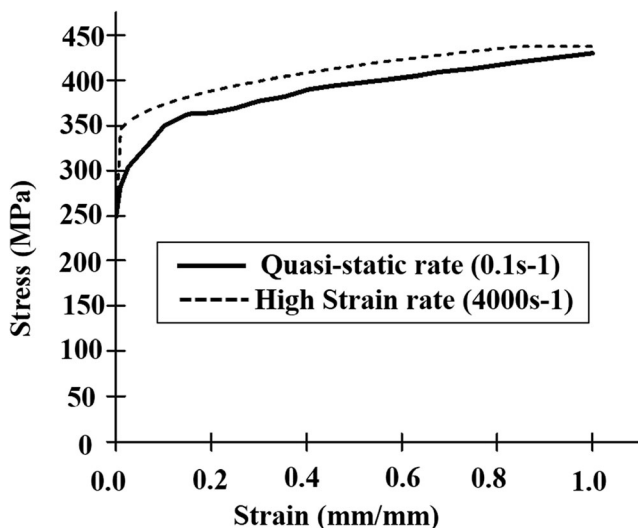


Fig. 1 Flow stress-strain curve of Aluminium alloy AA6061 at quasi-static and high strain rate [25, 26]

Table 1 Chemical composition of AA6061 [17]

Elements	Cu	Fe	Si	Mg	Mn	Al
Weight (%)	0.183	0.569	0.73	0.507	0.0924	Remaining

listed in Table 1. The mechanical and electrical properties of AA6061 and copper are given in Tables 2. Electrical conductivity of OFHC copper and AA6061 has been measured using conductivity meter of Technofour make (type 979).

2.2 Methods

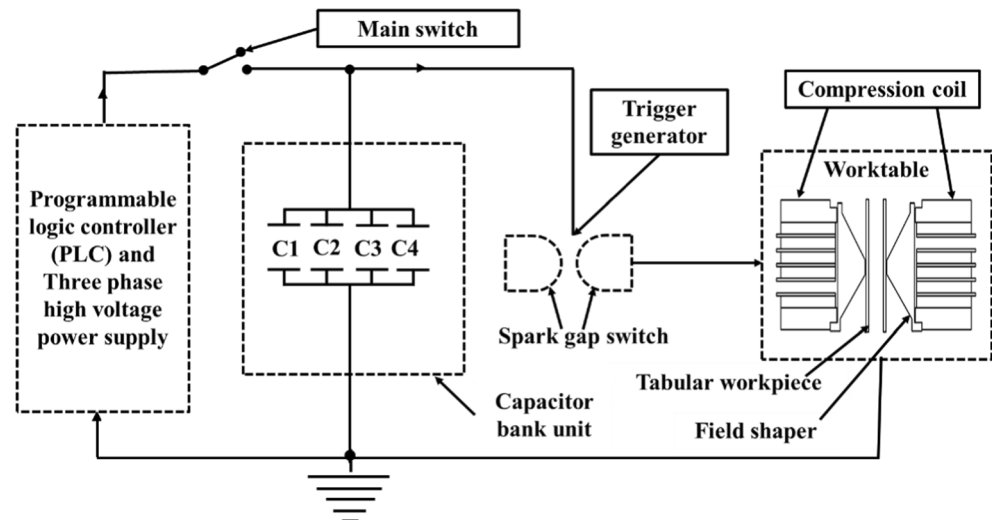
2.2.1 Experimental setup

A 40 kJ electromagnetic manufacturing (EMM) machine is used for forming of Al tube in the present work. A schematic line diagram of the electromagnetic forming setup is shown in Fig. 2 and a picture of the same is shown in Fig. 3. It mainly consists of four parts namely control console, capacitor bank rack, the programmable logic controller (PLC) rack and worktable (with discharge coil). The energy is stored in four capacitor banks and each capacitor bank has four capacitors of 56 μF capacity, so that the total capacitance of the machine is 224 μF . The control console is a human machine interface (HMI) that is used to select charging parameters such as the number of capacitor banks and charging voltage. So, it is also used to controls, visualize and select these parameters. The coil and other tooling are fastened on the worktable, and the workpiece is placed inside the coil for compression of a tube. There are two types of compression coil that is used, namely, bitter and solenoid helical coil. Both bitter and solenoid helical coils have the same application for compression of tubular geometries in electromagnetic forming. Solenoid helical coil can be used for application related to low energy application as its life is limited and fails after a few shots. To enhance the life of a coil, a bitter type of coil is used. It is developed using angular conducting plates, connected in sequence through a small piece of copper called sector. Solenoid helical coil is in the shape of helix. The reactionary stresses are high in case of solenoid helical coil and the coil fails after a period of time. In case of bitter coil structure, the coil has high strength and it

Table 2 Mechanical properties and electrical of Aluminium alloy AA6061 and OFHC copper [25, 27]

Material	Density (kg/m^3)	Poisson's ratio	Young Modulus (GPa)	Conductivity (ρ) S/m
AA-6061	2700	0.33	69	2.7×10^7
OFHC (Cu)	8960	0.34	124	5.88×10^7

Fig. 2 Schematic line diagram of circuit of electromagnetic forming machine



has high stress bearing capability. It can also produce strong magnetic field. Six turn bitter coil with field shaper is used in the present work. Details of the same are given in the next section. The output current pulse and associated parameters are measured with the Rogowski coil and digital storage oscilloscope of Tektronix make (model TPS 2024B). Current pulse is obtained in experiments through Rogoswki coil and amplitude and frequency are measured through digital storage oscilloscope. The capacitor banks are charged by high voltage DC supply from power supply rack and it stores power in the form of static charge. The stored energy is instantly released through a coil fixed on worktable. The discharge current produces a strong dynamic magnetic field around the coil (primary current). The change in flux of magnetic field induces an opposing effect in the nearby placed workpiece and an opposite direction current (secondary current) flows through the workpiece which produces opposing magnetic field. These two opposing magnetic field generates repulsive Lorentz force that accelerates the flyer workpiece to achieve desired shape. Charging of capacitors banks takes 5 to 15 s depending on the rate of charging, applied

energy/voltage, whereas it discharges through the coil in a very short time of 50–150 μ s.

2.2.2 Methodology

In the present work, coil geometry is varied with fixed geometry of field shaper and workpiece (tubular AA6061). The detailed dimensions of coil along with level of energy used for experimental work are listed in Table 3. The workpiece is 90 mm long with 24 mm outer diameter and 3 mm thickness. The effect of coil geometry variation on numerically calculated parameters and subsequently on the deformation of workpiece is correlated. Change in coil geometry such as PCD, cross section of turn (X) and effective turn (n) (as listed in Table 3) has effect on various parameters of electromagnetic forming process such as magnetic field, Lorentz force, velocity and displacement. The constant gap of 1 mm has been maintained between the coil and the field shaper. The same gap is also maintained between the field shaper and workpiece. Experiments are performed at different discharge energy levels such as 14 kV, 16 kV and 18 kV using two capacitor banks (2B) and FE simulation works are also carried at all

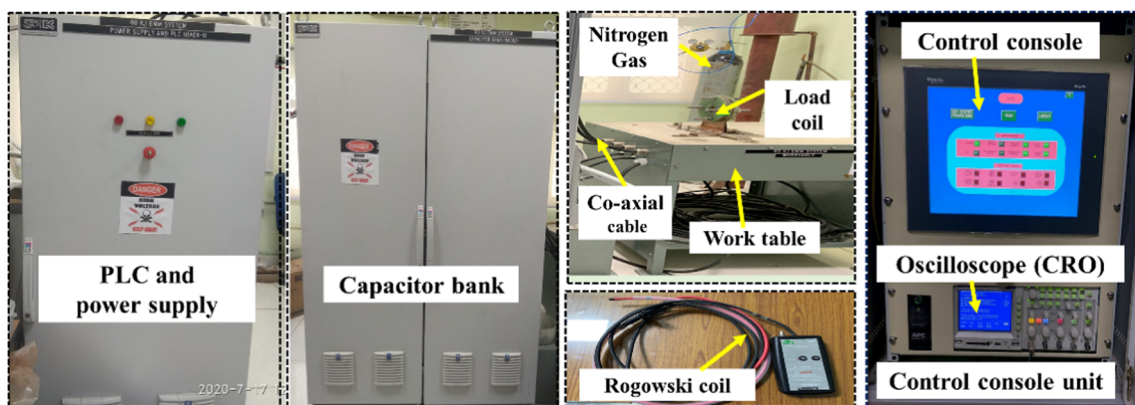


Fig. 3 Different components of electromagnetic forming (EMF) system used in experiments

Table 3 Details of coils and energy levels at which experiments are carried out

Coil	Area of cross section (X) (mm × mm)	Pitch circular diameter (PCD) (mm)	Effective turns (n)	Energy (E)/Voltage (kV) {Double bank (2B)}	Energy (E)/Voltage (kV) {Double bank (2B)}	Energy (E)/Voltage (kV) {Double bank (2B)}
A	8 × 64.5	155.5	4.23	18 kV	16 kV	14 kV
B	8 × 63	157	4.16	18 kV	16 kV	14 kV
C	8 × 58	152	4.16	18 kV	16 kV	14 kV
D	8 × 54.5	155.5	4.16	18 kV	16 kV	14 kV

conditions (as mentioned in Table 3). Fig. 4 shows schematic and actual picture of coil and field shaper respectively.

Analysis of EMF process to study the effect of coil geometry has been carried out using LS-DYNA finite element software. FEM model of the setup (coil, field shaper and tube) has been built up as per actual dimension. The model is meshed with 3D solid hexahedral element. Size of elements is 5 mm and it has been kept constant for both coil and field shaper. There is variation in number of elements for the coil because of variation in coil geometry as per Table 4. Coil A, B, C and D have 22386, 20696, 18240 and 16720 elements respectively. Field shaper has 5808 number of elements. Material properties as given in Table 2 and Fig. 1 have been assigned.

MAT_ELASTIC_001 card can be used to define material property like density, Young’s modulus and Poisson’s ratio for the elastic-plastic material (coil and field shaper) because this card supports deformation of material up to the elastic limit. Material properties assign through this card only for coil and field shaper because the generated stress across coil and field shaper has under elastic limit. Material model of EM_MAT_001 card is available in LS-DYNA software that is implemented to assign types of electromagnetic material and its properties like materials (conductor, insulator, air/vacuum) and electrical properties (conductivity for field shaper, coil and workpiece) in the FE simulation. The stress-strain flow curve at different strain rate (quasi-static, 0.1 s⁻¹ and high

Fig. 4 (a) Front view of assembly (Coil, field shaper and workpiece), (b) Sectional view of coil, (c) Field shaper, (d) 3D model of bitter coil used in the experiments

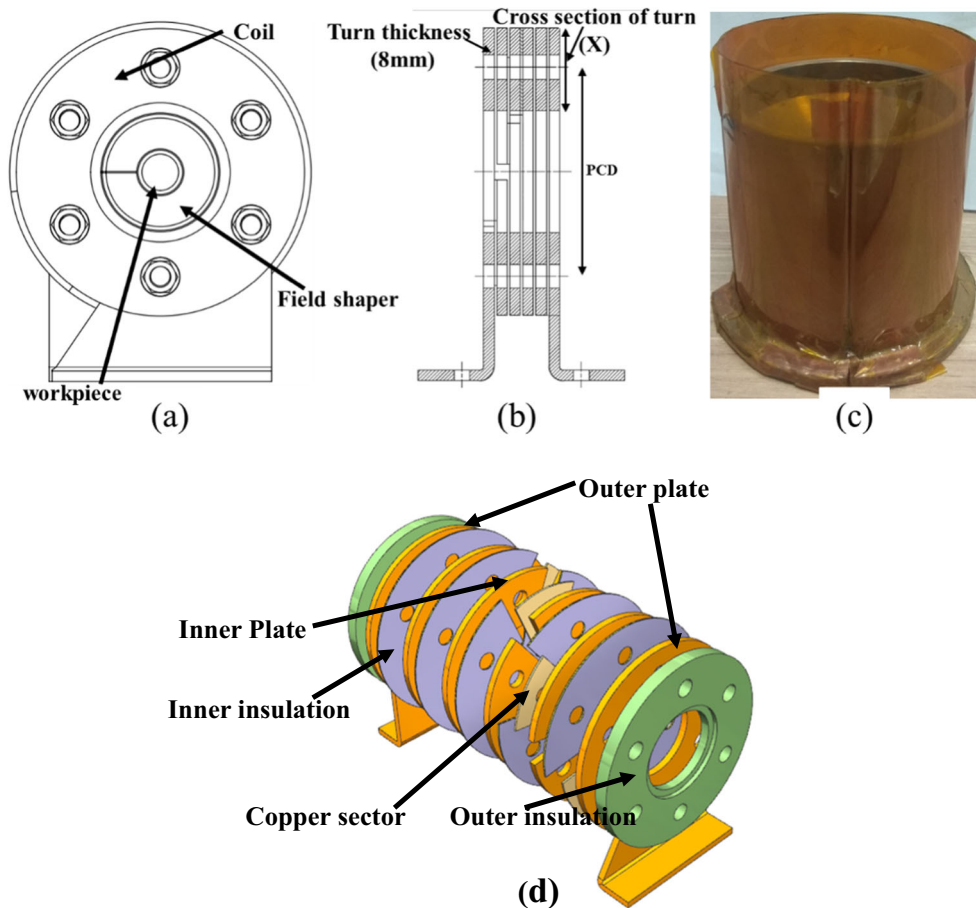


Table 4 Details of experimental and simulation using different coil at double bank 14 kV, 16 kV and 18 kV

Coil (voltage in kV)	Current (kA)	Frequency (kHz)	Initial OD (mm)	Final OD of tube (mm)		Difference in value of OD between experiments and FE simulation
				Experimental	Simulation	
A (14 kV)	110	10.4	24	17.5	20.34	2.84
A (16 kV)	132	11.6	24	16.91	18.8	1.89
A (18 kV)	140	11.6	24	16.4	16.8	0.4
B (14 kV)	120	12.20	24	17.33	19.95	2.62
B (16 kV)	140	12.5	24	15.7	17.96	2.26
B (18 kV)	155	12.5	24	15.2	15.62	0.42
C (14 kV)	112	11.11	24	18.5	20.93	2.43
C (16 kV)	132	11.6	24	16.84	18.72	1.88
C (18 kV)	144	11.6	24	16.4	16.72	1.32
D (14 kV)	104	10.4	24	19	21.86	2.86
D (16 kV)	120	10.6	24	18.06	20.5	2.44
D (18 kV)	136	10.6	24	17.6	18.08	0.48

strain rate, 4000 s^{-1}) for the workpiece (AA6061) tube shown in Fig. 1 has been used for FE simulation. In the commercial available LS-DYNA software, material model card MAT_24 (elasto-plastic material) is used to define the strain rate dependent material behaviour for the parts (tube) of the given FE model. If material (part) is deformed under low strain rate condition ($0.1/\text{s}$) during FE simulation, the material considers data from the low strain rate flow curve. Similarly, when material is deformed under high strain rate condition

($4000/\text{s}$) the material model takes data from high strain rate flow curve during the FE simulation [28]. The load is applied across coil in terms of current pulse using set segment feature of LS-DYNA. Experimentally determined current pulse corresponding to the level of voltage used in experiments is applied using EM_CIRCUIT_ROGO card across the coil terminals. Details of the current pulse obtained in experiments are discussed in next section. FEM model of the setup is shown in Fig. 5. Boundary

Fig. 5 FEM Model of (a) workpiece, (b) field shaper, (c) coil, and (d) all parts in assembled condition

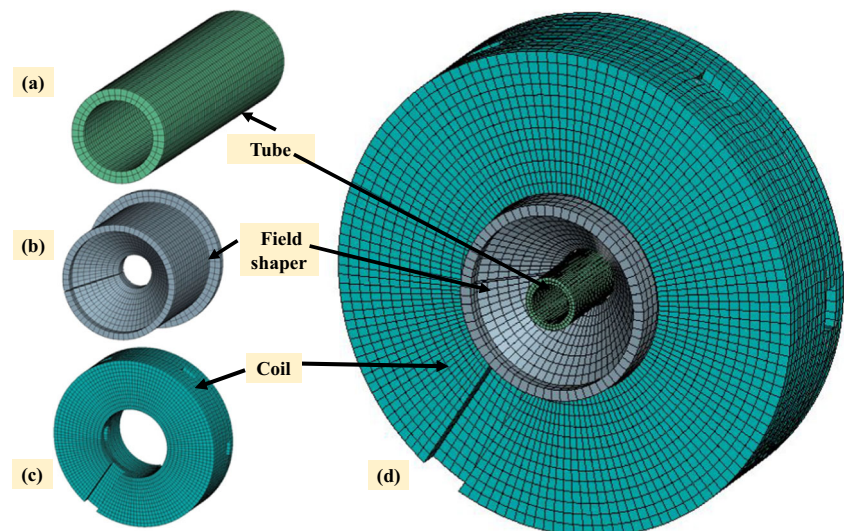
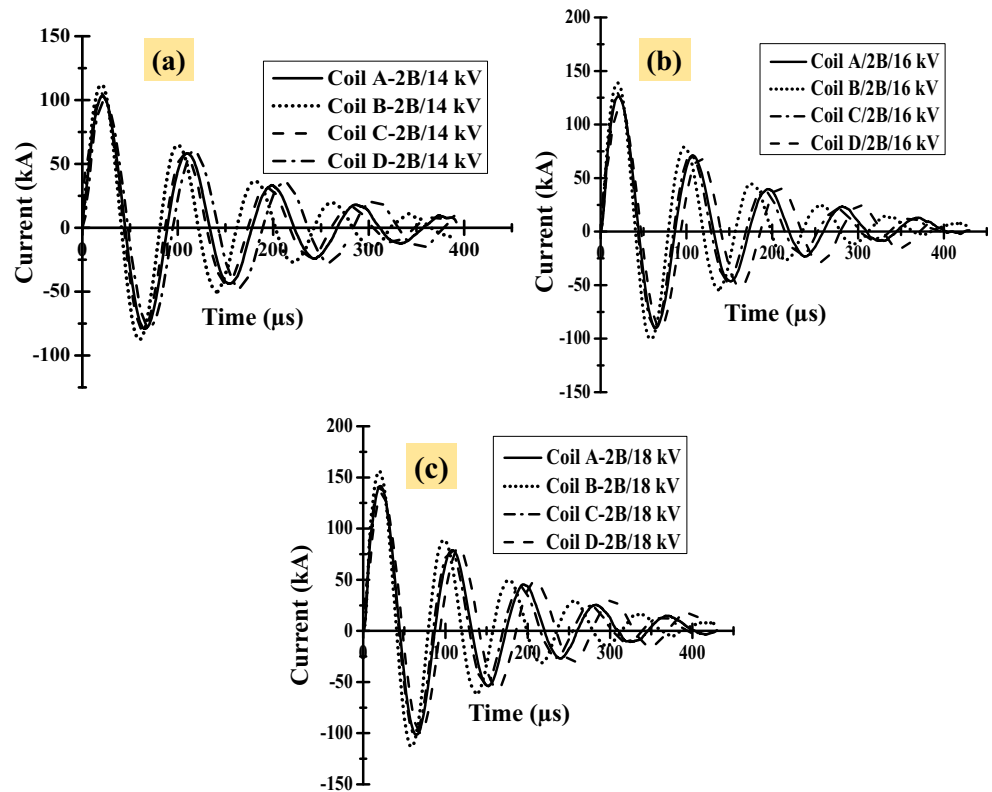


Fig. 6 Effect of different coil geometry on current pulse at double bank at (a) 14 kV, (b) 16 kV and (c) 18 kV



condition has been applied according to actual fastening condition used in experiments. In the experimental

setup, the tube is inserted inside the field shaper as shown in Figs. 4 (a) and 5 . The tube is rigidly fixed

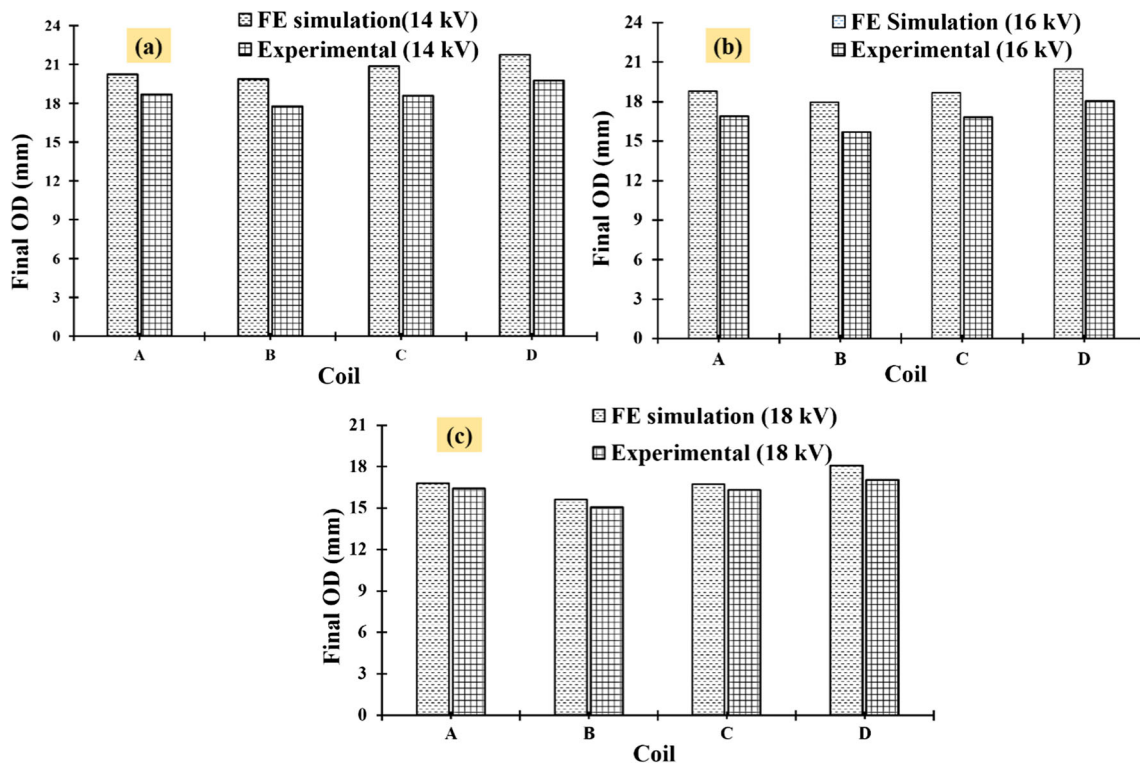
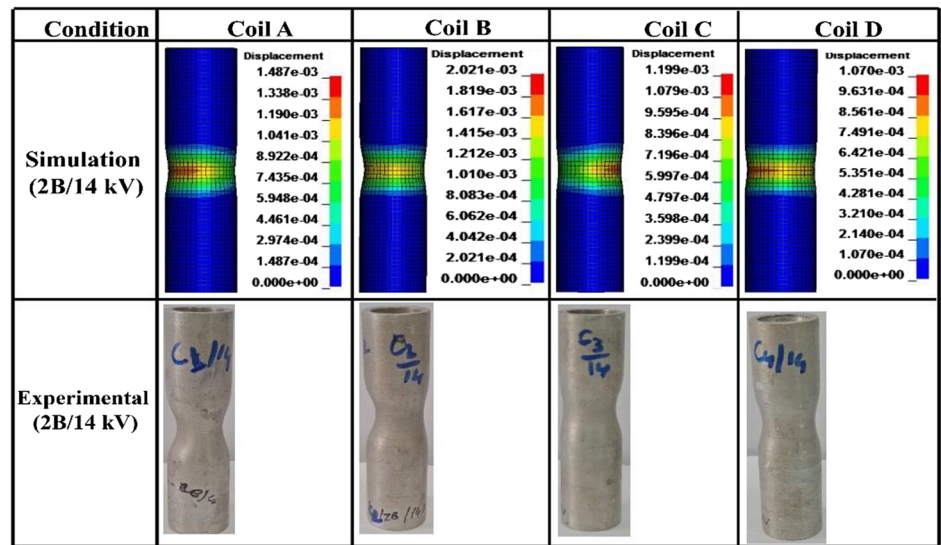
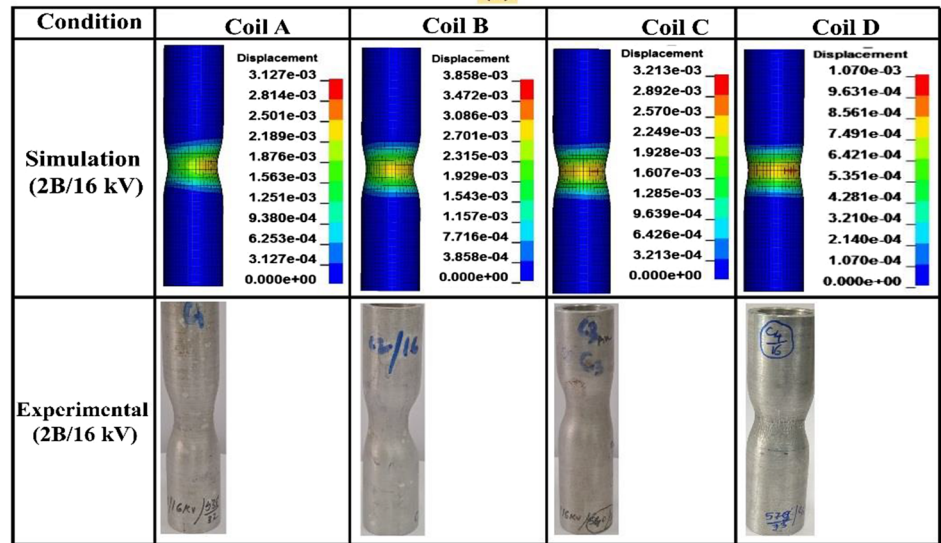


Fig. 7 Change in outer diameter of AA6061 tube for different coils using double bank at (a) 14 kV, (b) 16 kV, (c) 18 kV (Both experimental and simulation)

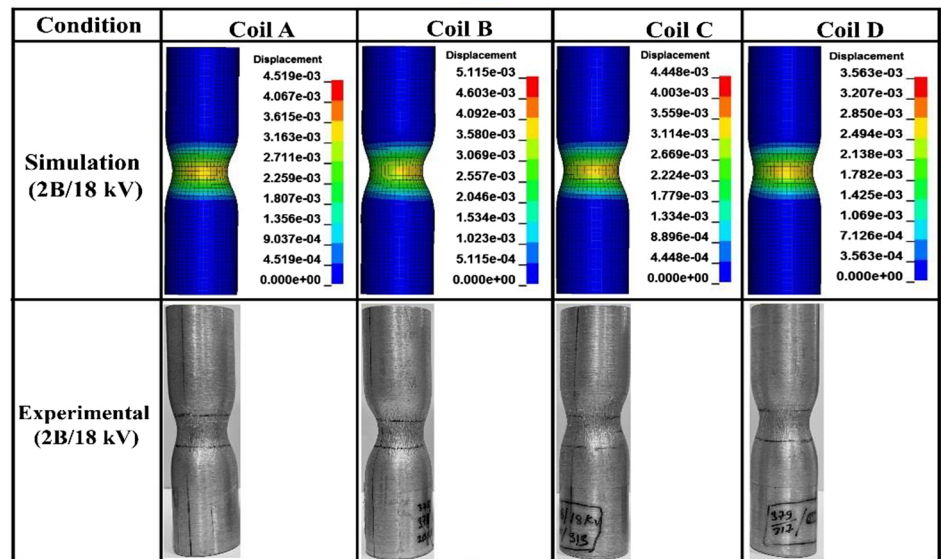
Fig. 8 Deformation of tube using different coil at (a) 14 kV, (b) 16 kV, and (c) 18 kV (experimental and simulation)



(a)



(b)



(c)

Table 5 Maximum value of process parameters in electromagnetic forming of AA6061 tube using different coils at 14 kV, 16 kV and 18 kV

Coil (voltage in kV)	Magnetic field (Tesla)	Lorentz force (GN/m ³)	Velocity (m/s)	Displacement (mm)	Stress (MPa)
A (14 kV)	10.82	130	102	1.87	381
A (16 kV)	12.5	189	183	2.6	401
A (18 kV)	13.9	231	250	3.6	413
B (14 kV)	11.25	153	136	2.02	389
B (16 kV)	13.4	222	234	3.02	409
B (18 kV)	15	275	308	4.19	424
C (14 kV)	10.92	132	103	1.53	385
C (16 kV)	12.7	192	190	2.64	403
C (18 kV)	13.9	229	252	3.64	415
D (14 kV)	10.7	119	90	1.07	371
D (16 kV)	12.1	156	119	1.75	387
D (18 kV)	13.7	207	191	2.96	404

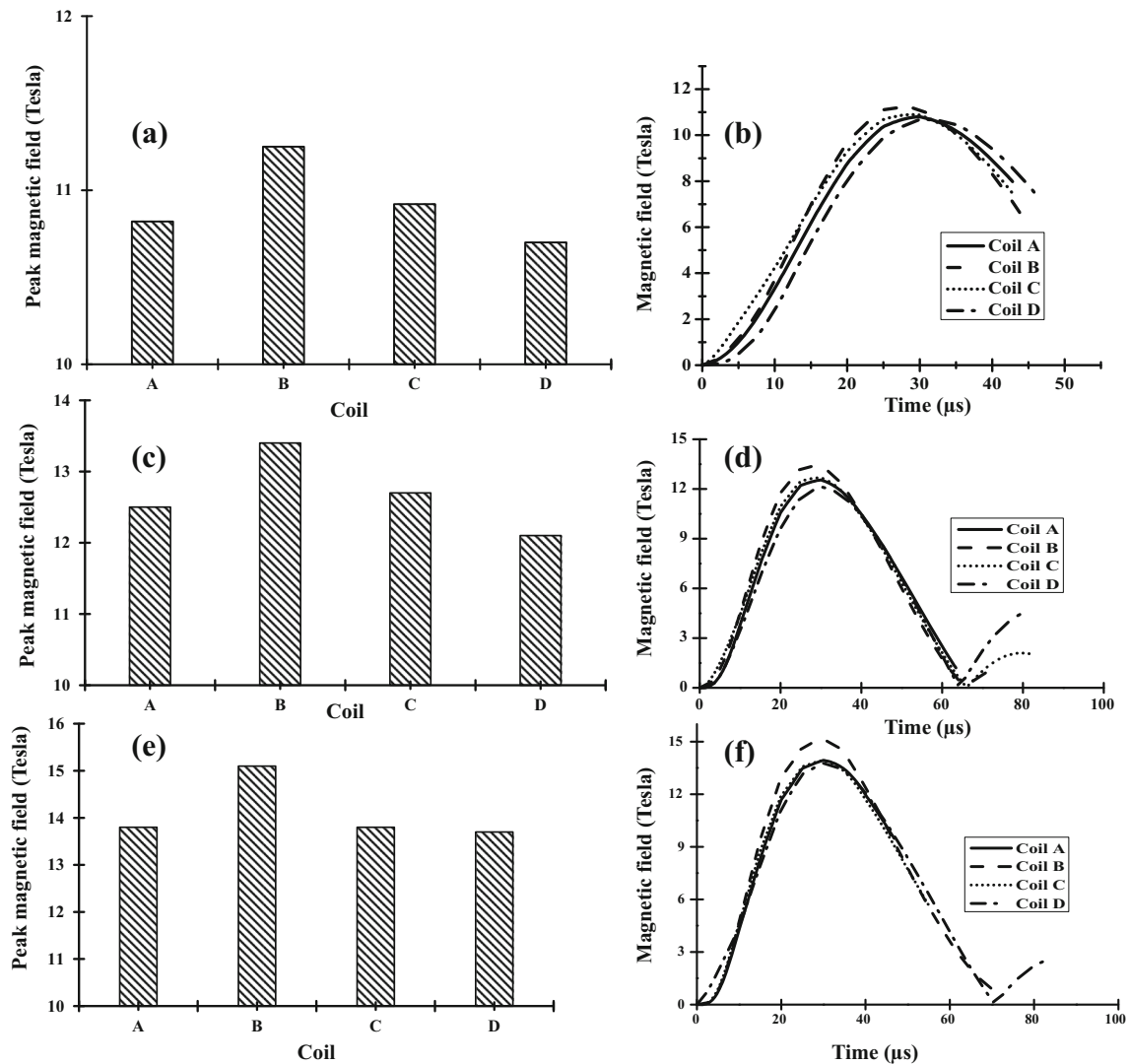


Fig. 9 Variation of magnetic field using different coils at 14 kV (a, b), 16 kV (c, d) and 18 kV (e, f)

by two supporting plate from both end of coil. The whole coil- field shaper- workpiece assembly is rigidly fixed on the table using the hole on the outer plate of the bitter coil (Fig. 4(d)). The FE model has been applied with similar boundary condition by defining a set node segment, a feature of LS-DYNA. The nodes of the defined set segment have been constrained for all six degree of freedom.

3 Results and discussion

Results of FEM simulation and corresponding experiments work have been discussed in this section. Comparative analysis (both numerical and experimental) of deformation of tube due to variation in coil geometry is carried out. Parameters which are difficult to determine experimentally are estimated

numerically and correlated with experimental deformation. The value of these numerically estimated parameters is taken from the outer layer of element/node of tubular workpiece located at the opposite to the slit of the field shaper. Result of current pulse and comparison of deformation of tube through experimental and FE simulation corresponding to all coils at 14 kV, 16 kV and 18 kV of energy levels are listed in Table 4. Peak value of current and frequency shows that coil B has the highest current and there is no change in frequency for the same coil even at different energy levels. So, frequency does not depend on energy of the system. The complete pulse of current for all coils at all the energy levels is shown in Fig 6. At all levels of energy, coil B given maximum peak value of current i.e. 120 kA, 140 kA and 155 kA at 14 kV, 16 kV and 18 kV respectively. It is obvious that highest current deforms the tube to the highest value as compared to lower current peak achieved by other coils. The same can be verified from both experimentally measured and numerically estimated final

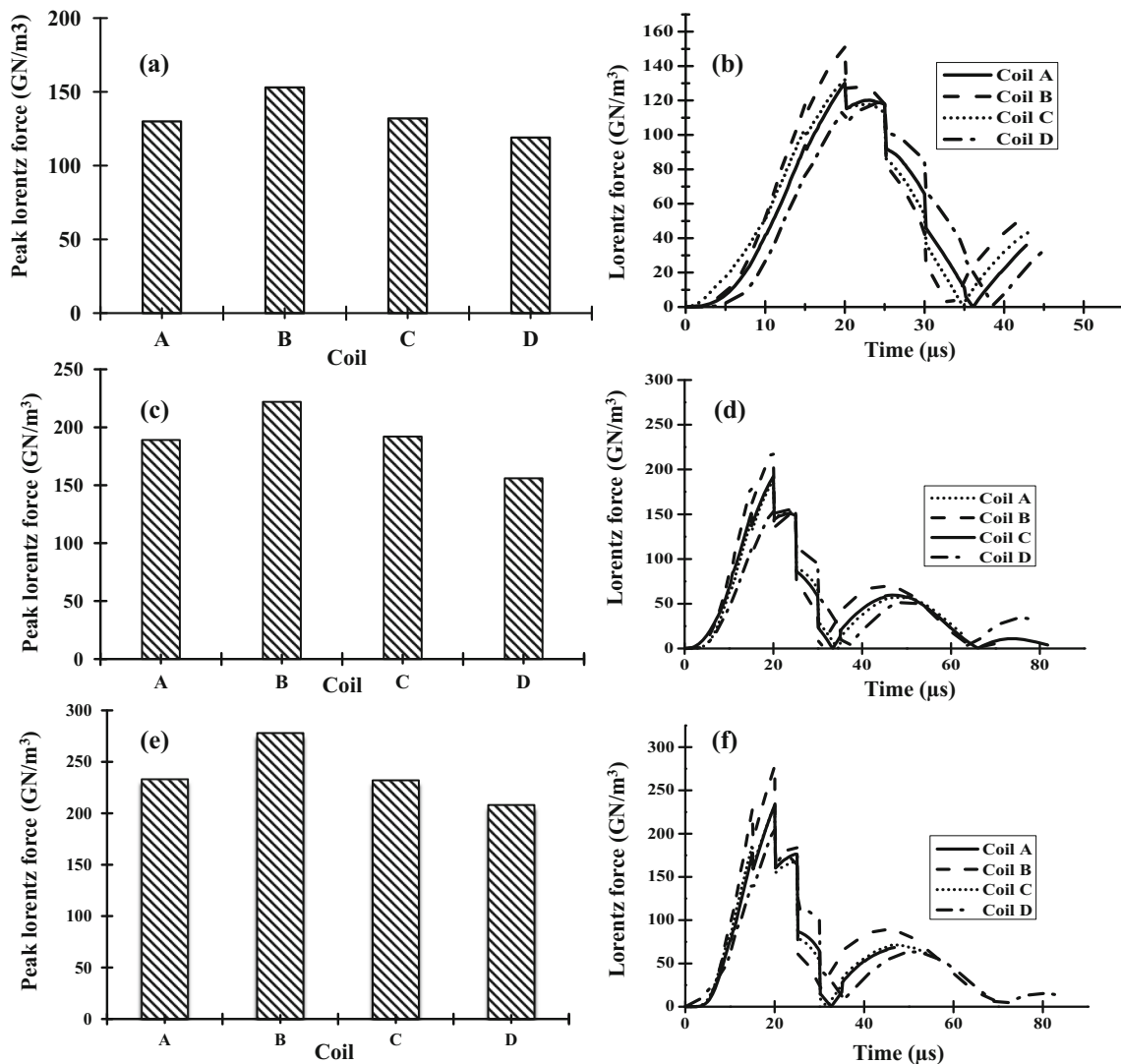


Fig. 10 Influence of different coil geometry on Lorentz force at double bank 14 kV (a, b), 16 kV (c, d) and 18 kV (e, f)

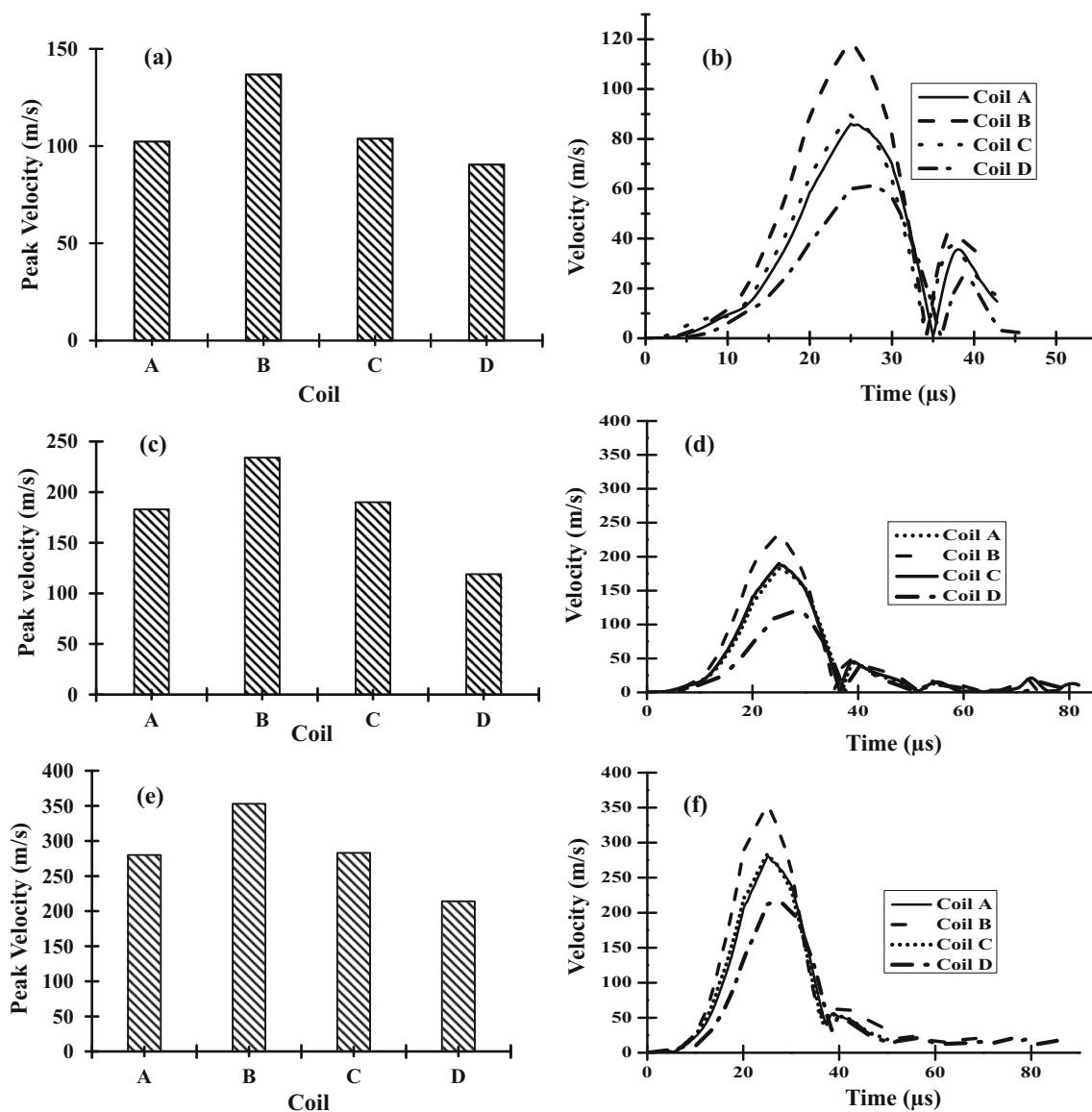
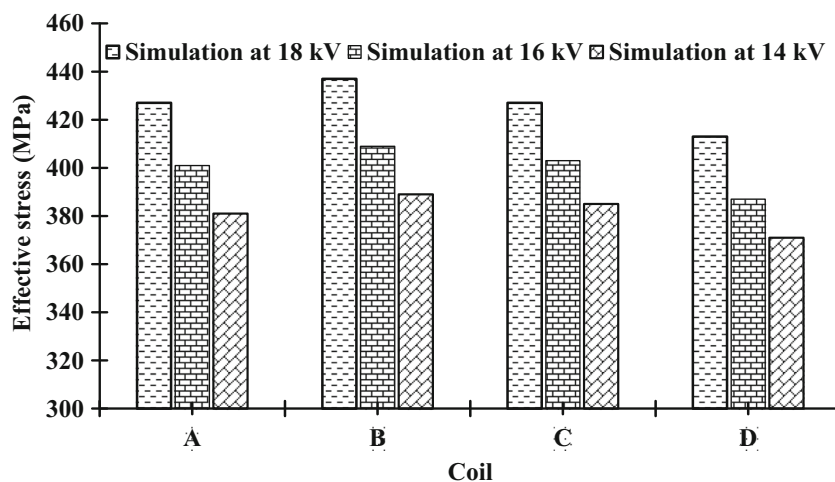


Fig. 11 Variation of velocity using different coils at 14 kV (a, b), 16 kV (c, d) and 18 kV (e, f)

outer diameter (OD) of tube as shown in Table 4. Measurement of experimentally deformed tube has been carried out using digital Vernier calliper. Measurement of OD of tube is taken at an angular location 90–270° where the slit of field shaper is assumed to be at 0°. Coil B reduces the outer (OD) to 15.2 mm and 15.62 mm from 24 mm in experimental and FE simulation. This is the highest deformation achieved amongst all coils at both energy levels. Experiments are conducted at all energy levels i.e., 14 kV, 16 kV and 18 kV energy levels. The comparison of experimental and numerical deformation shows very good agreement as the difference in the value is within ±3 mm. The comparison of peak value of current as shown in Fig. 6, shows that highest peak current is achieved by coil B followed by coil C, A and D. The comparison of coil geometry shows that coil B has

highest value of PCD amongst all coils and lower effective turns as compared to A. Both coil A and B have the same value of OD with just 3 mm difference in inner diameter (ID). So, it can be concluded that coil B has optimal condition combination of effective turns and turn cross section. So, the value of PCD, turn cross section and effective turns play important role in output current pulse. The turn cross section of coil B is lower than A. This indicates that the resistance of the coil B must be high as compared to coil A leading to high current but the results show opposite trends. It can be argued that the effective turn is a more dominant factor as it influences the inductance of the coil significant. It is a known fact that the value of inductance has more influence on discharge current pulse as well as frequency. Similar finding can be co-related by comparing effective turns in coil A

Fig. 12 Maximum value of effective stress (Von-Mises) after the deformation of AA-6061 tube when used the different types of coil condition at double bank 14 kV, 16 kV and 18 kV



and coil B. Coil B has lower number of effective turn that leads to higher value of current magnitude and frequency of current as compared to coil A. The comparison of values of PCD of coil A and D shows that they have the same value and it indicates that PCD hold minimal effect on the output performance of coil when compared to effective turn. Similarly, value of deformation in terms of OD of tube also shows the same trend and it is plotted in Fig. 7. Highest deformation is achieved by coil B at all energy levels. Results of FE simulation in terms of contour of displacement at all levels of energy for all the coils are shown in Fig. 8. The experimentally deformed tube sample at 14 kV, 16 kV and 18 kV is also shown in the figure. It shows very good agreement when experimentally deformed tube is compared with numerical one. The deformation has been compared by measuring the final OD of tube in both experimental and FE simulation. FE simulated final OD of tube was measured by selecting nodes of elements located at angle of 90° and 270° of tube using measure option in LS-DYNA. These locations are considered assuming the slit of the field shaper to be at 0° which is similar to conditions of measurement in experiments. It can also be verified pictorially that coil B deformed to maximum value as compared to other coils. Thus, the effect of coil geometry has been analysed by comparing deformation and pulse of the current.

The associated parameters (magnetic field, Lorentz force, velocity, displacement and stress) of electromagnetic forming which is difficult to measure/determine experimentally are estimated numerically and variation of their values for different coils is correlated. Data obtained through FE simulation can be represented in two ways: one only peak value and another variation of the parameter during whole duration of deformation. Maximum value of all numerically estimated parameter listed in Table 5. Comparative analysis of peak value and complete deformation duration of these parameters

are shown in Figs. 9, 10, 11, and 12. Variation of magnetic field at the centre of tube (opposite to the slit of field shaper) as calculated by FE simulation for all coils are shown in Fig. 9. Both peak value as well as its variation during deformation shows the same trend as shown by corresponding peak value of current. Coil B has highest value of magnetic field i.e., 15 T followed by C, A and D at all levels of energy. Similar trends can be seen for Lorentz force and velocity as seen in Figs. 10 and 11. The comparison of magnetic field to the nearest highest value which is produced by coil C shows an approximate variation of 1 T. There is a difference of approximately 1.5 T when effect of energy i.e. 14 kV, 16 kV and 18 kV is evaluated for all the coils. The peak value of velocity is 136 m/s, 234 m/s and 308 m/s for coil B at 14 kV, 16 kV and 18 kV respectively. This value is significantly high when compared to next level of three value i.e., 103 m/s, 190 m/s and 252 m/s for coil C. The importance of this magnitude of variation of velocity can be very significant when critical value of impact velocity is important to achieve in joining of two metals. The importance of the same is discussed by Kore et al. [29]. The comparison of maximum stress induced due to different coil reveals similar trend i.e. highest stress is induced by coil B as compared to all other coil as shown in Fig. 12. So, for all energy bank, selecting a suitable coil geometry is very crucial for workpiece deformation in electromagnetic forming for any application.

4 Conclusions

A study on the effect of variation in coil geometry on the deformation of the tube in electromagnetic forming process by experimental and numerical simulation is carried out in the present work. The numerical results are presented in terms of the magnetic field, velocity, Lorentz force, displacement and effective stress. The numerical simulation results are verified with experimental in terms of deformation of tube and a very

good agreement was observed. The finding of the present work is summarized below:

1. There is significant effect of PCD, turn cross-section and effective turns on deformation of tube.
2. Effective turns hold higher significance as compared to both PCD and turn cross-section of a compression coil. It can be argued that effective turns influence the inductance of the coil and turn cross section influence the resistance. It infers that the value of inductance has very important role in coil design and its performance in terms of output of the system or the deformation of workpiece/job.
3. The comparative analysis of tube deformation through experiments and simulation shows good agreement. Other parameters like magnetic field, velocity, Lorentz force, displacement and effective stress have been predicated numerically to correlate the findings. The experimental findings are in good agreement with numerically calculated trends of these parameters. Coil B shows maximum deformation experimentally and corresponding numerically predicated values of magnetic field, velocity, Lorentz force, displacement and effective stress are also the highest amongst all the coils. So, the FE analysis can be used to predict the performance of the coil by varying its effective number of turns, PCD and turn cross section before it is fabricated.

Acknowledgements The authors would like to thank Director, CSIR-AMPRI Bhopal for providing the facilities and CSIR New Delhi for support to perform this work.

Author contribution Manoj Soni: contributed in development of methodology, performed experiments and analysed results; Dr. Meraj Ahmed: conceptualized the proposed work and provided resources for experimental and simulation and supervised the work; Dr. Sanjay Kumar Panthi: suggested inputs for simulation and literature review; Dr. Surendra Kumar: contributed in preparation of samples, editing and writing paper; Khushwant Singh Gavel: contributed in finite element simulation.

Funding This work was funded by the Council of Scientific and Industrial Research (CSIR), New Delhi, India (Project no. MLP-0105).

Data and materials availability The data and supporting materials of the results of present work are available within the article. Data will be made available when requested.

Code availability Not applicable

Declarations

Ethics approval and consent to participate There is no ethical issue in the present work. Yes, there is consent from all authors to participate.

Consent for publication All co-authors declare their consent for publication of this work.

Competing interests All authors declare no competing interests.

References

1. Seth M, Vohnout VJ, Daehn GS (2005) Formability of steel sheet in high velocity impact. *J Mater Process Technol* 168(3):390–400. <https://doi.org/10.1016/j.jmatprotec.2004.08.032>
2. Golovashchenko SF (2007) Material formability and coil design in electromagnetic forming. *J Mater Eng Perform* 16:314–320. <https://doi.org/10.1007/s11665-007-9058-7>
3. Kalpakjian S, Sekar KV, Schmid SR (2001) Manufacturing engineering and technology. Pearson Education India, Delhi
4. Psyk V, Risch D, Kinsey BL, Tekkaya AE, Kleiner M (2011) Electromagnetic forming—a review. *J Mater Process Technol* 211:787–829. <https://doi.org/10.1016/j.jmatprotec.2010.12.012>
5. Baines K, Duncan J, Johnson W Electromagnetic metal forming. *Proc Instn Mech Eng* 1965, 180(1):93–110. https://doi.org/10.1243/PIME_PROC_1965_180_013_02
6. Lal G, Hillier M (1968) The electrodynamics of electromagnetic forming. *Int J Mech Sci* 10(6):491–500. [https://doi.org/10.1016/0020-7403\(68\)90030-1](https://doi.org/10.1016/0020-7403(68)90030-1)
7. Murata M, Suzuki H (1990) Profile control in tube flaring by electromagnetic forming. *J Mater Process Technol* 22(1):75–90
8. Min DK, Kim DW (1993) A finite-element analysis of the electromagnetic tube-compression process. *J Mater Process Technol* 38(1–2):29–40. [https://doi.org/10.1016/0924-0136\(93\)90183-7](https://doi.org/10.1016/0924-0136(93)90183-7)
9. Lee SH, Lee DN (1994) A finite element analysis of electromagnetic forming for tube expansion. *Transactions of the ASME-H- J Eng Mater Technol ASME(United States)* 116(2):250–254. <https://doi.org/10.1115/1.2904281>
10. Zhang H, Murata M, Suzuki H (1995) Effects of various working conditions on tube bulging by electromagnetic forming. *J Mater Process Technol* 48(1–4):113–121. [https://doi.org/10.1016/0924-0136\(94\)01640-M](https://doi.org/10.1016/0924-0136(94)01640-M)
11. Lee SH, Lee DN (1996) Estimation of the magnetic pressure in tube expansion by electromagnetic forming. *J Mater Process Technol* 57(3–4):311–315. [https://doi.org/10.1016/0924-0136\(95\)02086-1](https://doi.org/10.1016/0924-0136(95)02086-1)
12. Zhang H, Yang Z, Ren L (2019) Experimental investigation on structure parameters of E-shaped coil in magnetic pulse welding. *Mater Manuf Process* 34(15):1701–1709. <https://doi.org/10.1080/10426914.2019.1689263>
13. Meriched A, Féliachi M, Mohellebi H (2000) Electromagnetic forming of thin metal sheets. *IEEE Trans Magn* 36(4):1808–1811. <https://doi.org/10.1109/20.877796>
14. El-Azab A, Gamich M, Kapoor A (2003) Modeling of the electromagnetic forming of sheet metals: state-of-the-art and future needs. *J Mater Process Technol* 142(3):744–754. [https://doi.org/10.1016/S0924-0136\(03\)00615-0](https://doi.org/10.1016/S0924-0136(03)00615-0)
15. Haiping Y, Chunfeng L, Jianghua D (2009) Sequential coupling simulation for electromagnetic–mechanical tube compression by finite element analysis. *J Mater Process Technol* 209(2):707–713. <https://doi.org/10.1016/j.jmatprotec.2008.02.061>
16. Mamalis A, Manolakos D, Kladas A, Koumoutsos A (2006) Electromagnetic forming tools and processing conditions: numerical simulation. *Mater Manuf Process* 21(4):411–423. <https://doi.org/10.1080/10426910500411785>
17. Shrivastava A, Telang A, Jha A, Ahmed M (2019) Experimental and numerical study on the influence of process parameters in electromagnetic compression of AA6061 tube. *Mater Manuf Process* 34:1–12. <https://doi.org/10.1080/10426914.2019.1655156>
18. Ahmed M, Panthi S, Ramakrishnan N, Jha A, Yegneswaran A, Dasgupta R, Ahmed S (2011) Alternative flat coil design for electromagnetic forming using FEM. *Trans Nonferrous Metals Soc*

- China 21(3):618–625. [https://doi.org/10.1016/S1003-6326\(11\)60759-0](https://doi.org/10.1016/S1003-6326(11)60759-0)
19. Arezoodar AF, Haratmeh HE, Farzin M (2012) Numerical and experimental investigation of inward tube electromagnetic forming-electromagnetic study. *Advanced Materials Research*. Trans Tech Publ:6710–6716. <https://doi.org/10.4028/www.scientific.net/AMR.383-390.6710>
 20. Li F, Mo J, Zhou H, Fang Y (2013) 3D Numerical simulation method of electromagnetic forming for low conductive metals with a driver. *Int J Adv Manuf Technol* 64(9-12):1575–1585. <https://doi.org/10.1007/s00170-012-4124-1>
 21. Cao Q, Han X, Lai Z, Zhang B, Zhou Z, Qiu L, Li L (2013) Effects of current frequency on electromagnetic sheet metal forming process. *IEEE Trans Appl Supercond* 24(3):1–4. <https://doi.org/10.1109/TASC.2013.2279886>
 22. Dond S, Kulkarni M, Kumar S, Saroj P, Sharma A (2015) Magnetic field enhancement using field shaper for electromagnetic welding system. 2015 IEEE Applied Electromagnetics Conference (AEMC), IEEE, pp. 1-2. <https://doi.org/10.1109/AEMC.2015.7509219>
 23. Zeng X, Meng Z, Liu W, Huang S, Zhou S, Lin Y (2020) Electromagnetic forming of aluminum alloy strip by imposing inverse current instead of inducing eddy current. *Int J Adv Manuf Technol* 111:3481–3488. <https://doi.org/10.1007/s00170-020-06356-w>
 24. Savadkoohian H, Arezoodar AF, Arezoo B (2017) Analytical and experimental study of wrinkling in electromagnetic tube compression. *Int J Adv Manuf Technol* 93(1-4):901–914. <https://doi.org/10.1007/s00170-017-0571-z>
 25. Guo Y, Wen Q, Horstemeyer M (2005) An internal state variable plasticity-based approach to determine dynamic loading history effects on material property in manufacturing processes. *Int J Mech Sci* 47:1423–1441. <https://doi.org/10.1016/j.ijmecsci.2005.04.015>
 26. Shang J, Hatkevich S, Wilkerson L (2012) Comparison between experimental and numerical results of electromagnetic tube expansion. 12th International Ls-Dyna Users Conference Detroit, USA, pp. 1-10
 27. Johnson GR, Cook WH (1985) Fracture characteristics of three metals subjected to various strains, strain rates, temperatures and pressures. *Eng Fract Mech* 21:31–48
 28. Ls-DYNA Keyword User Manual, Volume I, May 2007, Version 971; Livermore Software Technology Corporation (LSTC), California, USA, 2007.
 29. Kore SD, Dhanesh P, Kulkarni SV (2010) Numerical modeling of electromagnetic welding. *Int J Appl Electromagn Mech* 32(1):1–19. <https://doi.org/10.3233/JAE-2010-1062>

Publisher's note Springer Nature remains neutral with regard to jurisdictional claims in published maps and institutional affiliations.